Chromatin Compaction at the Mononucleosome Level

ARTICLE *in* BIOCHEMISTRY · MARCH 2006

Impact Factor: 3.02 · DOI: 10.1021/bi052110u · Source: PubMed

3 AUTHORS, INCLUDING:

Katalin Tóth
German Cancer Research Center
58 PUBLICATIONS **954** CITATIONS
SEE PROFILE

Jörg Langowski
German Cancer Research Center
246 PUBLICATIONS **6,489** CITATIONS
SEE PROFILE

Chromatin Compaction at the Mononucleosome Level

Katalin Tóth,* Nathalie Brun, and Jörg Langowski

Division Biophysics of Macromolecules (B040), German Cancer Research Center, Im Neuenheimer Feld 580, D-69120 Heidelberg, Germany

Received October 17, 2005; Revised Manuscript Received November 23, 2005

ABSTRACT: Using a previously described FRET technique, we measured the distance between the ends of DNA fragments on which nucleosomes were reconstituted from recombinant and native histones. This distance was analyzed in its dependence on the DNA fragment length, concentration of mono- and divalent counterions, presence of linker histone H1, and histone modifications. We found that the linker DNA arms do not cross under all conditions studied but diverge slightly as they leave the histone core surface. Histone H1 leads to a global approach of the linker DNA arms, confirming the notion of a "stem structure". Increasing salt concentration also leads to an approach of the linker DNAs. To study the effect of acetylation, we compared chemically acetylated recombinant histones with histones prepared from HeLa cells, characterizing the sites of acetylation by mass spectroscopy. Nucleosomes from chemically acetylated histones have few modifications in the core domain and form nucleosomes normally. Acetylating all histones or selectively only H3 causes an opening of the nucleosome structure, indicated by the larger distances between the linker DNA ends. Selective acetylation of H4 distances the linker ends for short fragments but causes them to approach each other for fragments longer than 180 bp.

The conformation of chromatin in the living cell is strongly correlated with gene activity and is controlled by many physicochemical and biochemical factors. To elucidate the mechanism of this control, many in vitro analytical studies have been published where the compaction of isolated chromatin fibers and isolated or reconstituted oligonucleosomes was characterized by imaging (for a recent review, see ref *1*), solution scattering (*2*, *3*), or hydrodynamic methods (*4*, *5*). Slight changes in the ionic strengths of the environment and the presence of linker histones became apparent as important inducers of in vitro compaction. Moreover, the correlation between increased genetic activity and elevated levels of core histone acetylation makes it probable that acetylation and other histone modifications also play a central role in chromatin compaction. Since all of these factors influence the electrostatic landscape of the nucleosomes, we asked whether these changes might already be manifested at the mononucleosome level, e.g., by changing the geometry of the linker DNA arms.

The ionic environment is the most studied parameter influencing chromatin compaction. Although one can hardly imitate in vitro the intracellular environment, typical compact and open chromatin fibers are reproducibly isolated and may be interconverted by varying the type and concentration of monovalent and divalent salts (*6*). The fiber compactness is characterized by its diameter as measured on electron micrographs. Values of around 30 and 10 nm are typical for the compact and loose conformation. The 30 nm fiber form is reached above 20−50 mM monovalent ion concentration or with more than 0.2 mM Mg^{2+} ions (*6*). Salt-dependent compaction has been reproduced also on di- or trinucleosomes. Here a decrease of the internucleosomal distances and angles has been observed by hydrodynamic and microscopic methods between 5 and 20 mM NaCl without further compaction at higher concentrations (*7*−*9*). Our neutron small angle scattering data indicate even a further compaction up to 100 mM NaCl (*10*). These results imply salt-induced closing of the linker DNA arms in oligonucleosomes. We aim to study this effect here on mononucleosomes, where only an unfolding effect of very low ionic strength (below 1 mM) was reported earlier (*11*, *12*).

Another well-studied inducer of compaction is the linker histone. In the absence of linker histones only few examples of compact chromatin structures exist in nature. Knockout experiments have shown that linker histones are not essential for cell viability, but their absence modifies the size and structure of the nuclei (*13*). In vitro chromatin condensation can be obtained even in their absence, but regularly compacted stable structures need the correct attachment of stoichiometric amounts of linker histones (*14*). How the linker histones modify the path of the linker DNA is seen on cryo-electron microscopy images: a stem structure could be observed on mono- and oligonucleosomes (*15*, *16*). Our FRET[1] distance measurements on reconstituted mononucleosomes at low ionic strength (5 mM NaCl) have already shown that the incorporation of H1 linker histone decreases the distance between the linker arms over their whole length (*17*). This paper investigates further this effect in combination with the other compaction factors.

The general view for more than 30 years has been that histone acetylation is correlated with increased genetic activity and that hyperacetylation sometimes correlates with

* Corresponding author. Phone: 49-6221-423390. Fax: 49-6221-423391. E-mail: kt@dkfz.de.

[1] Abbreviations: FRET, fluorescence resonance energy transfer; bp, base pairs; TAU gel, Triton−acetate−urea gel.

10.1021/bi052110u CCC: $33.50
Published on Web 01/20/2006

cancer. However, the structural basis of the effect is not known yet. The degree and sites of acetylation vary widely with cell type and cell cycle phase. Acetylation is found to be moderate in the presence of H1 linker histones (*18*). An arsenal of histone acetyltransferases (HATs) and deacetylases has been discovered, and several antibodies helped to identify their sites of action. Most of the naturally acetylated sites were identified as lysines on the N-terminal tails of the core histones, the most important being those on the H3 and H4 tails. Recent studies showed, however, an acetylation of lysine 91 in the globular part of histone H4 (*19*). The exact path and DNA contacts of the histone tails are not yet known, but it has been shown that without tails the chromatin compaction is not correct (*20*). It was postulated that histone tails play a role in the nucleosome−nucleosome interaction either directly or through the linker DNA. Due to the known charge neutralization upon acetylation, it was suggested that these interactions would be weakened and consequently the chromatin structure should open locally, allowing access for different enzymes and transcription machines. Whether charge neutralization alone can induce the observed biological effects has not yet been analyzed.

Despite early expectations based on gel retardation differences (*21*), the global structural parameters of isolated or reconstituted chromatin fibers failed to show significant changes upon hyperacetylation. Hydrodynamic parameters of mono- or oligonucleosomes do not change upon acetylation in the presence of H1 (*22*), but decreased compactness is measured for acetylated oligonucleosomes in the absence of H1 (*23*). This last observation correlates with electron microscopic results by the same authors. The thermal stability of acetylated oligo- and mononucleosomes (*24*), as well as the mechanical stability as measured by stretching (*25*), is slightly decreased. The α helicity of the H4 histone tail increases upon acetylation (*26*, *27*) and so is responsible for small CD changes found in acetylated nucleosomes (*22*). Nevertheless, the interaction of the H4 tail with the linker DNA persists even after acetylation, as shown by UV cross-linking experiments (*28*). Acetylation does not affect the capacity of histones to form oligonucleosomes (*29*, *30*), the nucleosome repetition length, and the rate of H1 incorporation (*31*). Acetylation is not indispensable for chromatin remodeling (*32*), but ATP-dependent remodeling is found to be more effective on acetylated chromatin fibers (*33*). The DNA of the chromatin-containing hyperacetylated histones shows some interesting features. Upon histone acetylation, a significant but small increase is observed in equilibrium accessibility of very different parts of the nucleosomal DNA (*34*), and its DNase sensitivity and flexibility are also increased (*31*).

Most of the above-mentioned observations were obtained with chromatin isolated from hyperacetylated cells or reconstituted by hyperacetylated octamers, in both cases all four core histones being more or less acetylated. One other complication is that the acetylases may also act on non-histone proteins, and their acetylation effect is sometimes inseparable from other posttranslational histone modifications. To study the effect of selective acetylation of the different core histones, we have acetylated the recombinant histones chemically prior to nucleosome reconstitution. This approach has the advantage that we can have the nonacetylated states as a comparison and we can acetylate the histones selectively. A second benefit is that other histone modifications do not influence our comparison. The disadvantage is that the chemically acetylated sites are not necessarily the same as those acetylated in vivo. To account for such differences, isolated hyperacetylated and less acetylated "normal" octamers of HeLa cells were compared.

The combination of the effect of acetylation, ionic conditions, and the presence of linker histones on the path of the linker DNA was measured with fluorescence resonance energy transfer, using double end-labeled fragments as in our earlier work (*17*).

MATERIALS AND METHODS

DNA Fragments. DNA fragments from 150 to 223 base pairs increasing in 10−11 bp steps, containing the nucleosome positioning sequence of the *Xenopus borealis* 5S ribosomal RNA gene in the center, were prepared by PCR amplification (template kindly provided by S. Dimitrov, Grenoble). The primers were labeled through a C6 carbon linker on their 5′ end either with rhodamine X (Thermo Hybaid GmbH, Ulm, Germany) or with Alexa 488 (in our laboratory). The PCR products were HPLC-purified (ion-exchange column Gen-Pak FAX, Waters) until they showed only one band on a polyacrylamide gel, either by ethidium staining or by direct fluorescence of the label. After buffer exchange on a NAP-5 column (Pharmacia), fragments were concentrated to 0.1−0.5 mg/mL in a vacuum centrifuge (Uniequip) and stored at −20 °C in TE buffer (10 mM Tris, pH 7.5, 0.1 mM EDTA) containing 5 mM NaCl. Nonlabeled and single-labeled DNAs of the same sequences were similarly prepared.

Histones. Recombinant core histones of *Xenopus laevis* were expressed in *Escherichia coli* as described in refs *35* and *36*. The isolation from the exclusion bodies and purification were performed as described in ref *36*. The four histones were lyophilized and stored separately at −80 °C. The histones were acetylated individually by incubating with 0.1 M acetyl phosphate (Sigma) at 1 mg/mL histone concentration for 3 h at 50 °C in TE-β buffer (10 mM Tris-HCl, pH 7.4, 0.1 mM EDTA, 0.5 mM β-mercaptoethanol).

Octamers were prepared from recombinant core histones containing all histones in nonacetylated form, all histones acetylated, or only H4, H3, or both H3 and H4 acetylated. Prior to octamer formation, equimolar concentrations of the four histones were unfolded by dissolving in unfolding buffer (7 M guanidine hydrochloride, 20 mM Tris-HCl, 10 mM dithiothreitol) or repeated buffer exchange by Vivaspin 20 (MWCO 10000) centrifugation. After 30 min of unfolding, the octamers were formed during an overnight dialysis against refolding buffer (TE-β with 2 M NaCl) in Slide-A-Lyser cassettes (MWCO 7000, Pierce) at 4 °C. Aggregates were separated by 5 min centrifugation at 5000 rpm followed by FPLC separation of tetramers and other smaller fragments (*36*).

For comparison, histone octamers were isolated from normal and hyperacetylated HeLa cell nuclei and purified in nonacidic conditions of the histones as described in our previous paper (*17*). Hyperacetylation was achieved by incubating the cells for 6 h with 6 mM sodium butyrate.

Linker histone H1 from calf thymus was purchased from Roche Diagnostics (Mannheim, Germany) and used after

purification on Sepharose and a NAP-5 column (Pharmacia, Germany). Aliquots of histone H1 were stored at −80 °C in TE buffer containing 5 mM NaCl and 0.5 mM PMSF.

The quality of the histone preparations was controlled on a silver-stained 18% SDS−polyacrylamide gel. Comparison with nucleosomes isolated from natural chromatin (COS-7 cells) showed that in our preparations all histones were present in equimolar concentrations and without degradation. The degree of acetylation was controlled on silver-stained Triton−acetic acid−urea (TAU) gel run overnight with a maximum of 30 mA at room temperature (*37*).

Nucleosome Reconstitution. Histone octamers and DNA fragments were mixed in TE buffer at 2 M NaCl concentration. Typical reaction volumes were 50−100 μL; the DNA fragment concentration was 0.4 μM. The DNA:octamer proportion varied between 1:1.8 and 1:2.2, as optimized for every histone preparation. The reconstitution was started for 30 min in silanized sterile Eppendorf tubes at room temperature; then it was dialyzed at 4 °C against stepwise decreasing concentrations of NaCl down to 5 mM in minidialyzing tubes (Pierce). If H1 was to be incorporated, it was added at 0.6 M NaCl concentration.

The quality of the reconstitution was checked with gel electrophoresis either on 6% polyacrylamide gel (60:1 acrylamide:bisacrylamide) in TBE buffer at 10 V/cm or on 2% agarose gel in 0.5× TBE buffer at 10 V/cm. Gels were stained by ethidium, and a video image was taken on an UV transilluminator. The video images were quantified using the program IQ (Bio Image), taking into account that the emission of ethidium is about 30% weaker in the case of nucleosomes than for free DNA (*38*). To demonstrate the incorporation of H1 linker histone, we looked for the slowing down of the migration of nucleosomes in agarose gel and also made MNase digestion. MNase (Roche Diagnostics, Mannheim, Germany) was added at 5 units/mL to the nucleosome solutions. Digestion by MNase was done in the presence of 1 mM $CaCl_2$ for different incubation times at 25 °C and was stopped by EDTA. The length of the nondigested DNA fragments was analyzed on 8% PAGE (29:1) after phenolization.

Absorption and Emission Spectra. For all measurements the samples were thermostated at 20 °C. Quartz cuvettes with a path length of 3 mm were silanized in order to avoid adhesion of the dye or proteins. Sample concentrations below 0.5 μM were used to avoid inner filter effect in the fluorescence measurements. Absorption spectra were measured on a Cary 4E spectrometer (Varian, Mulgrave, Australia) between 220 and 750 nm, with an absorbance accuracy of 0.001. Fluorescence emission spectra were measured with an SLM-AMINCO 8100 fluorescence spectrometer (SLM, Urbana, IL) using a 150 W xenon lamp. Emission spectra were collected between 500 and 750 nm with 4 nm monochromator slit width for excitation and emission. Excitation wavelengths were 495 nm for the donor and 585 nm for the acceptor. Spectra were measured relative to the lamp intensity and corrected for the instrument response and buffer signal. Numerical treatment of the collected data was done with the Kaleidagraph program. Integrated spectral regions were used for the determination of the energy transfer efficiency. The integration extended over ±5 nm in the absorption spectra and ±10 nm in the emission spectra. Fluorescence resonance energy transfer (FRET) efficiency was determined from the enhanced emission of the acceptor.

Determination of the FRET Efficiency and the Dye-to-Dye Distance. Two emission spectra were recorded for the calculation of the FRET efficiency at between 500 and 750 nm with excitations at 495 and 585 nm, respectively. The integrated emissions (I_1 and I_2) around the maxima 520 and 610 nm of the first spectrum and around 610 nm of the second spectrum (I_3) were used in the calculations. The measured I_2 is the sum of the enhanced emission (EE), the tail of the donor emission (*T*), and the emission from direct excitation (*D*) of the acceptor. Measuring I_1 and I_2 on a donor-only labeled sample, one can calculate the ratio of the maximum to the tail $F_T = I_1/I_2$, which is a constant. It is then used to calculate the hidden tail from the measured I_1 for every sample: $T = I_1/F_T$. Similarly, a factor $F_D = I_3/I_2$ measured on an acceptor-only labeled sample is used to calculate the hidden direct emission of the acceptor $D = I_3/F_D$.

The relative absorption at the excitation wavelength (495 nm) of the donor and acceptor molecules in the complex was taken from the absorption ratio of the acceptor at its maximum and at the excitation wavelength in single-labeled double-stranded DNA: $F_A = \{A_A^{585}\}/\{A_A^{495}\}$. In the absorption spectra of the double-labeled double-stranded DNA samples the measured absorption at the fluorescence excitation wavelength A^{495} is the sum of the donor and acceptor absorptions $A^{495} = A_D^{495} + A_A^{495}$. Their proportion is calculated from the measured absorptions on the double-labeled samples:

$$A_D^{495}/A_A^{495} = (A^{495}/A^{585})F_A - 1 \quad (1)$$

The efficiency of the energy transfer is then

$$\mathrm{ET} = \frac{I_2 - T - D}{D}\left(\frac{A_A^{495}}{A_D^{495}}\right) \quad (2)$$

expressed through the measured values and the proportion factors:

$$\mathrm{ET} = \frac{I_2 - I_1/F_T - I_3/F_D}{(I_3/F_D)[(A^{495}/A^{585})F_A - 1]} \quad (3)$$

Using HPLC-purified labeled primers and a second HPLC step after PCR preparation, we were able to estimate the double labeling of our DNA fragments as 100%. A small part of the fragments usually did not form nucleosomes. This fraction was quantified by gel analysis, and the measured ET was corrected for it. Only samples with less than 25% free DNA were measured.

The averaged dye-to-dye distance *R* is determined through the Förster radius R_0:

$$R = R_0\sqrt[6]{1/\mathrm{ET} - 1} \quad (4)$$

The factors F_T and F_D are independent of the salt environment whereas F_A and R_0 change slightly; the salt dependence of F_A was measured and taken into account in the calculations. The salt-dependent R_0 values were determined relative to the low salt R_0 from the overlap integrals, using measured donor quantum yields and emission spectra of double-labeled

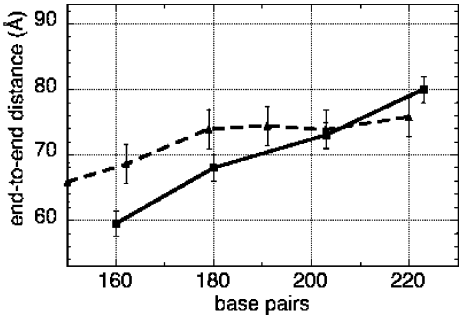

FIGURE 1: Dependence of the end-to-end distance of the nucleosomal DNA on the fragment length, calculated from FRET measurements. Nucleosomes were prepared from recombinant histones (solid line) and from isolated histone octamers of HeLa cells (dashed line).

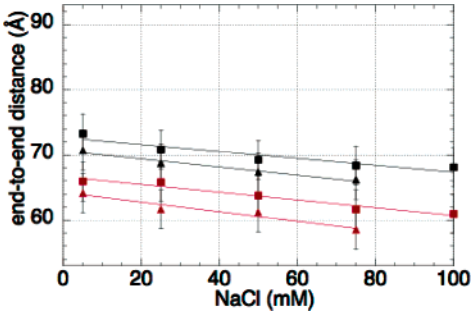

FIGURE 2: Effect of NaCl concentration on the linker DNA end-to-end distances in the absence (black) and presence (red) of linker histone H1. Values were calculated from FRET measurements on nucleosomes prepared from 203 bp (squares) and 171 bp (triangles) long DNA fragments.

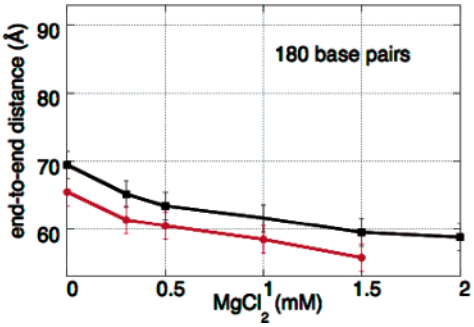

FIGURE 3: Effect of $MgCl_2$ on the linker DNA distances in the absence (black) and presence (red) of linker histone H1. DNA fragments of 180 bp were used.

160 bp long DNA fragments in the respective buffers. The slight increase of the refractive index was also taken into account. The orientation factor was controlled through the anisotropy of the bound dyes and was found to be insensitive to salt in the studied range. The calculated R_0 value decreased from 55 to 52.8 Å by increasing the NaCl up to 200 mM.

To exclude samples with eventual aggregation presenting an internucleosomal FRET, we controlled the flatness of the absorption spectra outside the absorption bands for each sample and the proportion of the Rayleigh band relative to the fluorescence in the fluorescence spectra.

As presented above, the ET values contain measured data from two spectra and from one gel quantification, as well as several constants. The errors were calculated from parallel measurements for several (5−10) preparations and were found to be below 0.5 nm in the dye-to-dye distance. Possible errors in the calculation factors did not affect the relative changes.

The measured FRET values are averages on a whole sample. Distance fluctuations of the dyes may appear from different sources: the largest are due to asymmetric positioning; on smaller scales the mobility of the longer linker DNAs plays a role and lastly the dye mobility. Due to the R^6 dependence of the FRET the average is strongly weighted for the shorter distances, so our R-values can be regarded as lower limits.

RESULTS AND DISCUSSION

No Crossing of the Linker DNAs. Nucleosomes were reconstituted from recombinant histones and DNA fragments of different lengths. The linker DNA end-to-end distance of the samples was then determined by FRET in low salt (5 mM NaCl) and also after addition of concentrated NaCl to more elevated concentrations. Figure 1 shows as example the linker end-to-end distance of nucleosomes reconstituted on DNA fragments of different lengths at low salt (5 mM NaCl) from recombinant and isolated histone octamers. It may be seen that the distance between the linker DNA ends increases monotonically, which means that, similarly to our earlier studies done with histone octamers isolated from HeLa cells (*17*), the linker DNAs of the mononucleosomes prepared here from recombinant histones diverge without apparent crossing. The data for all of the other experimental conditions, shown below, confirm this finding. This result is in good agreement with recent studies on the higher order structure of chromatin fibers (*39*) and tetranucleosomes (*40*).

Salts Lead to a Moderate Approach by the Linker DNAs. Increasing salt concentrations lead to a monotonic decrease of the dye-to-dye distances, corresponding to an approach of the linker DNAs for all different fragment lengths, with or without linker histones and for all acetylation states of the core histones. An example for two DNA fragment lengths with and without linker histones is given in Figure 2. Mg^{2+} causes this approach at much smaller concentration, as shown in Figure 3. This effect confirms the decrease of the electrostatic repulsive interaction of the linker DNAs due to the charge neutralization by the counterions. The measured distances do not allow a construction of a unique spatial path for the linker DNAs, but even in the more compact form our distance data are only compatible with a noncrossing geometry as was described earlier for low salt conditions (*17*).

The increase of the salt concentration showed two side effects: the ratio between nucleosome to free DNA decreased monotonically with the salt concentration, and at some stage the samples began to aggregate, disturbing the optical measurements. Both effects varied depending on the linker DNA length and the type of the histone octamers. We could observe these effects with recombinant and isolated octamers and not only the reconstituted, but also isolated nonfluorescent mononucleosomes of HeLa cells showed disintegration and aggregation in function of the NaCl concentration. We assume that this salt-dependent disintegration is due to the low nucleosome concentration ($<0.5\ \mu$M) as proposed earlier (*41*) and not as an artifact of reconstitution or octamer refolding. The disintegration was observed and quantified by agarose gel electrophoresis (Figure 4) and was taken into account by the calculation of the FRET value. Aggregation

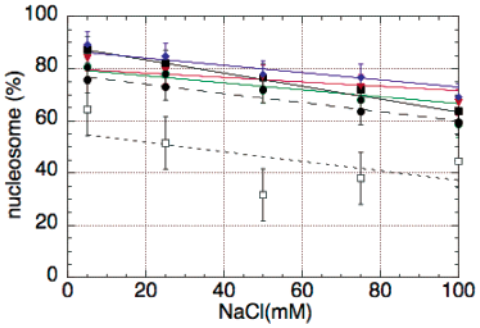

FIGURE 4: Nucleosome disintegration by increasing NaCl concentration calculated from agarose gel images. The nucleosome concentrations were between 300 and 800 nM. Nucleosomes were reconstituted from recombinant histones without modification (black solid line), with acetylation of H3 histone (green), H4 histone (blue) only, all histones (red), and from histone octamers isolated from HeLa cells (black dashed line) as well as isolated nonlabeled nucleosomes from HeLa cells (black dotted line).

was detected in the absorption spectrum through the increased baseline, and those samples were centrifuged or eliminated.

Compaction by Salts and by Linker Histones Is Additive. As earlier demonstrated for nonrecombinant histones at low salt (*17*), incorporation of linker histone H1 induces an approach of the linker DNA arms in mononucleosomes at all different fragment lengths and already at low salt concentration, as seen by the strongly increased FRET signal. A further slight approach is observed by increasing the ionic strength, similar to the case without linker histones (Figure 2). H1 incorporation was confirmed by gel retardation shift and MNase digestion stop at approximately 170 bp, proving the correct positioning (data not shown). Both of these methods are qualitative so we cannot tell whether the incorporation is fully stoichiometric, but we observed a monotonic increase of the incorporated H1 as a function of the added concentration and used the highest nonaggregating H1 concentration. We could observe under these conditions that the DNA closing effect of salts and linker histone go in the same direction.

Effects of Histone Acetylation on Nucleosome Compaction. Analysis of Histone Acetylation. Electrophoresis on TAU gel was used for separating histones with different acetylation states (Figure 5). The annotation of the bands was done according to ref *37*. In the lanes of the acetylated octamers we observed a weakening (H4) or total disappearance (H2A) of the nonacetylated bands and the appearance of several (three to six) differently acetylated fractions, corresponding to observations seen when the acetylation is performed by enzymes.

The gel also shows that the recombinant histones are not totally uniform, a second slower fraction of H4 and H2B being clearly seen above the nonacetylated bands and less visibly separated but present for the other two slower histones as well. The migration speed of these fractions correlates with that of the singly acetylated histones. Recombinant histones received from other laboratories presented this shift as well. Since there is no evidence in the literature for acetylation or other types of histone modification in bacteria, mass spectrometry was used to investigate this effect. Reflectron-in-source decay (reISD) experiments have shown a shift of 43 Da for the N-terminal residues in part of all

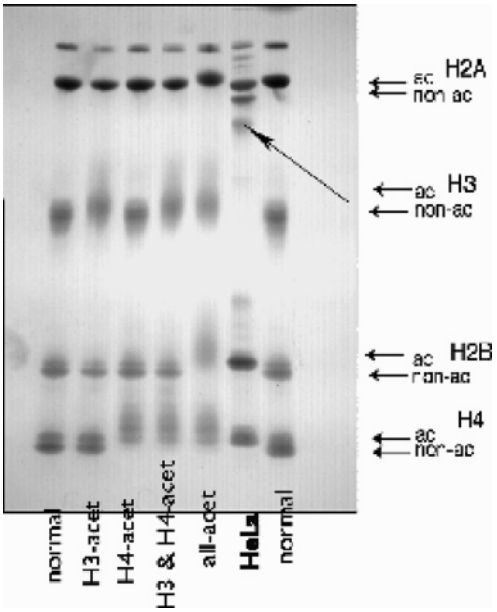

FIGURE 5: Characterization of histone octamer acetylation states by TAU (Triton−acetate−urea) gel. From left to right, lanes 1 and 7 contain octamers of unmodified recombinant histones. In lane 2 only histone H3 is acetylated, in lane 3 only H4, in lane 4 histones H3 and H4, and in lane 5 all four core histones. In lane 6 is isolated histone octamer from HeLa cells.

four recombinant histones (*42*). This could correspond to a carbamylation of these termini; a purification artifact neither excluded nor reported yet for recombinant histones. It seems that this modification does not affect the octamer- and nucleosome-forming capacity of the histones. In the mass spectra of isolated normal and hyperacetylated HeLa octamers, the shift is not present.

Using reISD spectra on solution of single histones, we could analyze the proportion of once or several times acetylated species and we could then specify the most probable sites of acetylation in the first 50 amino acids separately on the N- and C-termini (*42*). We found that the acetylation occurs mostly on the N-terminus (up to five lysines), whereas at most one lysine is modified at the inner C-terminus. In comparison, analysis of HeLa H4 histone revealed one acetylated and one dimethylated lysine at the N-terminus on the normal samples and only one additional acetylation for the hyperacetylated samples. The site of this biochemical acetylation is the same in the entire sample, contrary to the statistical distribution upon chemical acetylation. On the other hand, the chemical acetylation allows a comparison between purely nonacetylated and histone-selectively acetylated cases without any other modification. Further mass spectrometry from differently acetylated gel bands is under way.

On the basis of these results we are confident that the chemical acetylation is an adequate method for the study of specific effects of the selective acetylation of the different histones, although not of site-specific acetylation.

Chemical Acetylation Does Not Impede Nucleosome Formation. Figure 6 shows a native agarose gel of nucleosomes formed with differently acetylated recombinant histones using the same 223 bp DNA fragment. We have not found any significant difference in the efficiency of histone incorporation as seen in the ratio of the free DNA and nucleosomes. On the other hand, the relative proportion of

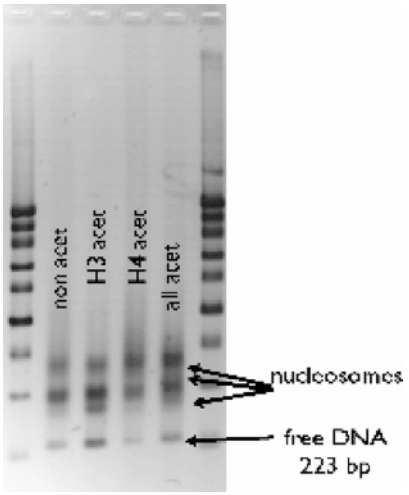

FIGURE 6: Agarose gel analysis of nucleosome reconstitution from differently acetylated recombinant histones and 223 bp DNA. From left to right, lanes 1 and 6 contain 100 bp DNA markers, lane 2 contains samples prepared with nonmodified recombinant histones, lane 3 with H3, and lane 4 with H4 acetylated, and in lane 5 all four histones were acetylated.

the differently retarded nucleosome bands depends strongly on the acetylation. It has been shown earlier (*43*) that for mononucleosomes the gel retardation depends on the symmetry of the positioning of the octamer. In the case of nucleosomes with linker DNAs of the length used here, asymmetrically positioned nucleosomes move faster due to the longer mobile DNA part. We observed that the octamers containing acetylated H3 form more of these faster migrating nucleosomes. The faster migration can be explained by a more asymmetric localization or reduced contact between DNA and histones. Incomplete nucleosomes containing only histone tetramers migrate also faster, but under our conditions this would result in a much faster band (data not shown).

The Linker DNA Distance Is Influenced by Histone Acetylation. This influence is very complex, depends on which histone is acetylated, differs depending on the fragment length, and is influenced by the surrounding ionic conditions. Figure 7A presents the end-to-end distance of the nucleosomal linker DNA as a function of the fragment length at 5 mM NaCl. For the 160 bp fragment where the DNA ends are close to the histone core, we find that acetylation of any histone opens the DNA arms. The extent of this opening depends on the acetylated histones: the effect of H4 acetylation is weaker than that of H3. Extending from the core, the geometry change depends on the acetylated histone: with H4 acetylated the linker arms stay even closer than with nonacetylated histones; with H3 or all histones acetylated the opening is more pronounced. The effect of the acetylation of H3 only or of all histones is similar above 180 base pairs, suggesting that H3 dominates over the H2A and H2B histones in determining the linker DNA path. Figure 7B shows the end-to-end distances obtained at 100 mM NaCl. Compared to low salt conditions, the closing effect of acetylated H4 begins already for shorter DNAs, closer to the histone core. The salt-dependent compaction of the differently acetylated nucleosomes for short (160 bp) and longer distances (223 bp) is plotted on Figure 8. We observed that the slopes are very similar for the different acetylation states and DNA lengths; thus the charge reduction of the

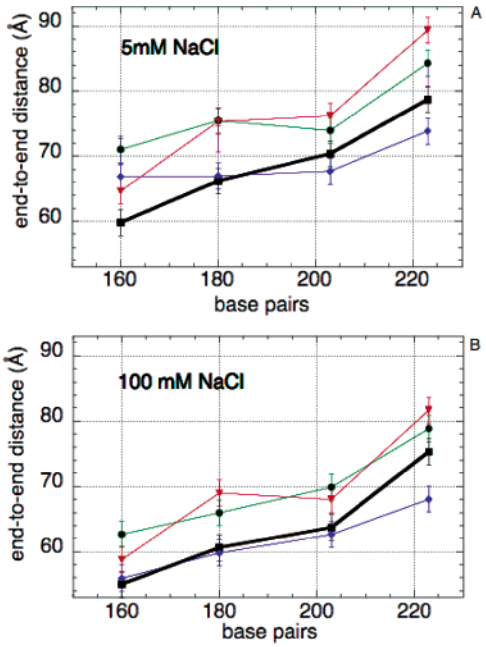

FIGURE 7: Dependence of the linker DNA end-to-end distances on the length of the DNA fragments. Nucleosomes were reconstituted from recombinant unmodified octamers (black) and from octamers where only histone H3 was acetylated (green) or only histone H4 (blue) as well as where all histones were acetylated (red). Values are presented from measurements in low salt, 5 mM NaCl (A), and in high salt, 100 mM NaCl, concentration (B).

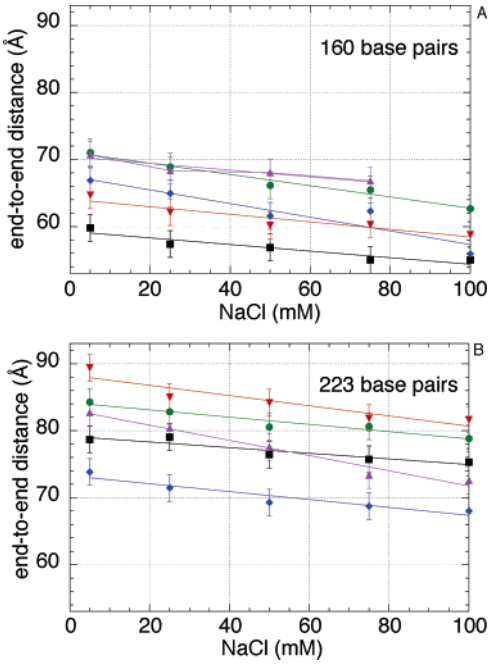

FIGURE 8: Dependence of the linker DNA end-to-end distances on the NaCl concentration for short DNA fragments of 160 bp (A) and for long DNA fragments of 223 bp (B). Purple symbols represent nucleosomes containing acetylated H3 and H4 histones; the other colors are the same as for Figure 7.

histones does not seem to interfere much with the electrostatic interaction of the linker DNA arms.

Figure 9 gives an overview of all data: we observe that the DNA diverging from the core as well as the salt-induced linker DNA closing are independent of the acetylation state and that the acetylation of H4 histone has a special closing effect on the distant DNA parts. The effect of histone H1

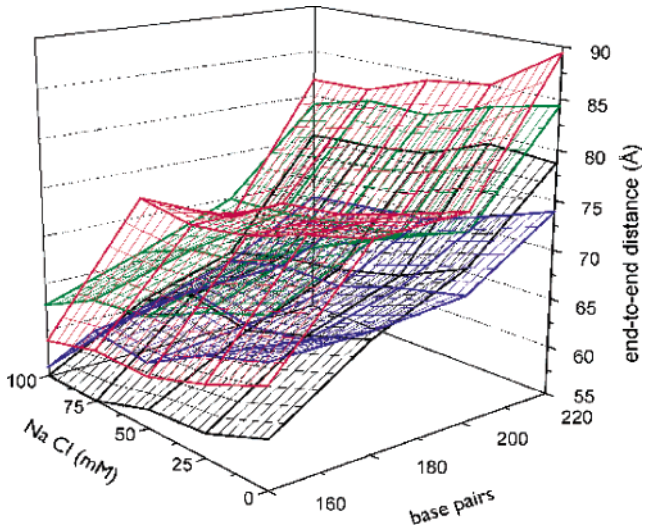

FIGURE 9: Dependence of the DNA end-to-end distances on the DNA length, salt concentration, and acetylation state of the recombinant histones. The color code is the same as for Figure 7.

on the linker DNA is not influenced significantly by the acetylation (data not shown).

The distance of the DNA linker arms is predominantly determined by the electrostatic DNA−DNA repulsion and by its shielding through the positive ions and the proximity of the histones. The increased distance by acetylated H3 can be explained by the neutralization of the positive tails. This can be regarded as an elementary step for chromatin decompaction through DNA repulsion. The decreased DNA distance in the case of acetylated H4 histone corresponds to a compaction. This necessitates looking for some other, more direct interaction between the linker DNA and the H4 histone tail.

What may explain the different effects of H3 and H4 acetylation? The tails of H3 histone are longer and protrude closer to the beginning of the linker DNA, whereas the shorter H4 tails start further from the DNA. We recall the observations that the distance between the H4 tail and linker DNA seems not to change upon acetylation and, furthermore, that the H4 tail shortens due to increased α helicity. The distances obtained for nucleosomes of HeLa histones (Figure 1) are most comparable with that of the H4-only acetylated sample. With histones isolated from butyrate-treated HeLa cells, the distances are in general 3−5 Å higher than for normal HeLa cells (not shown). Further studies are underway to characterize the effect of posttranslational histone modifications on nucleosome structure by FRET and mass spectrometry.

CONCLUSION

The studies presented here show that besides the effects of salt and linker histone binding, histone acetylation profoundly influences chromatin structure at the mononucleosome level. Global histone acetylation, or acetylation of H3 only, leads to an opening of the nucleosome structure in agreement with the observed chromatin fiber opening. In contrast, acetylation of H4 causes a more complex behavior where the linker DNA arms seem to open up only locally and actually approach each other more closely when they are further from the histone core. Such differential effects may play an important role in determining the precise function of histone modifications, and their further characterization will advance our understanding of the histone code. To elucidate the structural changes on the mononucleosome level in more detail, bulk FRET measurements have the disadvantage that only an average distance can be measured. Single molecule FRET studies on mono- and trinucleosomes are underway to overcome this limitation.

ACKNOWLEDGMENT

We thank Martina Schnölzer, Wilma Dormeyer, and Anja Resemann for the mass spectrometry measurements and interpretations. We also thank Walter Blass for help with the final rephrasing of the manuscript.

REFERENCES

1. Horowitz-Scherer, R. A., and Woodcock, C. L. (2004) Visualization and 3D structure determination of defined sequence chromatin and chromatin remodeling complexes, *Methods Enzymol. 376*, 29−48.
2. Graziano, V., Gerchman, S. E., Schneider, D. K., and Ramakrishnan, V. (1994) Histone H1 is located in the interior of the chromatin 30-nm filament, *Nature 368*, 351−354.
3. Graziano, V., Gerchman, S. E., Schneider, D. K., and Ramakrishnan, V. (1996) Neutron scattering studies on chromatin higher-order structure, *Basic Life Sci. 64*, 127−136.
4. Hansen, J. C., and Turgeon, C. L. (1999) Analytical ultracentrifugation of chromatin, *Methods Mol. Biol. 119*, 127−141.
5. Ausio, J. (2000) Analytical ultracentrifugation and the characterization of chromatin structure, *Biophys. Chem. 86*, 141−153.
6. van Holde, K. E. (1989) *Chromatin*, Springer, Heidelberg.
7. van Holde, K., and Zlatanova, J. (1995) Chromatin higher order structure: Chasing a mirage?, *J. Biol. Chem. 270*, 8373−8376.
8. Butler, P. J., and Thomas, J. O. (1998) Dinucleosomes show compaction by ionic strength, consistent with bending of linker DNA, *J. Mol. Biol. 281*, 401−407.
9. Yao, J., Lowary, P. T., and Widom, J. (1990) Direct detection of linker DNA bending in defined-length oligomers of chromatin, *Proc. Natl. Acad. Sci. U.S.A. 87*, 7603−7607.
10. Hammermann, M., Toth, K., Rodemer, C., Waldeck, W., May, R. P., and Langowski, J. (2000) Salt-dependent compaction of di- and trinucleosomes studied by small-angle neutron scattering, *Biophys. J. 79*, 584−594.
11. Wu, H. M., Dattagupta, N., Hogan, M., and Crothers, D. M. (1979) Structural changes of nucleosomes in low-salt concentrations, *Biochemistry 18*, 3960−3965.
12. Libertini, L. J., and Small, E. W. (1987) Reversibility of the low-salt transition of chromatin core particles, *Nucleic Acids Res. 15*, 6655−6664.
13. Shen, X., Yu, L., Weir, J. W., and Gorovsky, M. A. (1995) Linker histones are not essential and affect chromatin condensation in vivo, *Cell 82*, 47−56.
14. Carruthers, L. M., Bednar, J., Woodcock, C. L., and Hansen, J. C. (1998) Linker histones stabilize the intrinsic salt-dependent folding of nucleosomal arrays: mechanistic ramifications for higher-order chromatin folding, *Biochemistry 37*, 14776−14787.
15. Furrer, P., Bednar, J., Dubochet, J., Hamiche, A., and Prunell, A. (1995) DNA at the entry-exit of the nucleosome observed by cryoelectron microscopy, *J. Struct. Biol. 114*, 177−183.
16. Bednar, J., Horowitz, R. A., Grigoryev, S. A., Carruthers, L. M., Hansen, J. C., Koster, A. J., and Woodcock, C. L. (1998) Nucleosomes, linker DNA, and linker histone form a unique structural motif that directs the higher-order folding and compaction of chromatin, *Proc. Natl. Acad. Sci. U.S.A. 95*, 14173−14178.
17. Tóth, K., Brun, N., and Langowski, J. (2001) Trajectory of nucleosomal linker DNA studied by fluorescence resonance energy transfer, *Biochemistry 40*, 6921−6928.
18. Gunjan, A., Sittman, D. B., and Brown, D. T. (2001) Core histone acetylation is regulated by linker histone stoichiometry in vivo, *J. Biol. Chem. 276*, 3635−3640.
19. Ye, J., Ai, X., Eugeni, E. E., Zhang, L., Carpenter, L. R., Jelinek, M. A., Freitas, M. A., and Parthun, M. R. (2005) Histone H4 lysine 91 acetylation a core domain modification associated with chromatin assembly, *Mol. Cell 18*, 123−130.

20. Fletcher, T. M., and Hansen, J. C. (1995) Core histone tail domains mediate oligonucleosome folding and nucleosomal DNA organization through distinct molecular mechanisms, *J. Biol. Chem. 270*, 25359−25362.
21. Krajewski, W. A., Panin, V. M., and Razin, S. V. (1993) Acetylation of core histones causes the unfolding of 30 nm chromatin fiber: analysis by agarose gel electrophoresis, *Biochem. Biophys. Res. Commun. 196*, 455−460.
22. Ausio, J., and van Holde, K. E. (1986) Histone hyperacetylation: its effects on nucleosome conformation and stability, *Biochemistry 25*, 1421−1428.
23. Garcia-Ramirez, M., Rocchini, C., and Ausio, J. (1995) Modulation of chromatin folding by histone acetylation, *J. Biol. Chem. 270*, 17923−17928.
24. Yau, P., Thorne, A. W., Imai, B. S., Matthews, H. R., and Bradbury, E. M. (1982) Thermal denaturation studies of acetylated nucleosomes and oligonucleosomes, *Eur. J. Biochem. 129*, 281−288.
25. Brower-Toland, B., Wacker, D. A., Fulbright, R. M., Lis, J. T., Kraus, W. L., and Wang, M. D. (2005) Specific contributions of histone tails and their acetylation to the mechanical stability of nucleosomes, *J. Mol. Biol. 346*, 135−146.
26. Wang, X., Moore, S. C., Laszckzak, M., and Ausio, J. (2000) Acetylation increases the alpha-helical content of the histone tails of the nucleosome, *J. Biol. Chem. 275*, 35013−35020.
27. Siino, J. S., Yau, P. M., Imai, B. S., Gatewood, J. M., and Bradbury, E. M. (2003) Effect of DNA length and H4 acetylation on the thermal stability of reconstituted nucleosome particles, *Biochem. Biophys. Res. Commun. 302*, 885−891.
28. Mutskov, V., Gerber, D., Angelov, D., Ausio, J., Workman, J., and Dimitrov, S. (1998) Persistent interactions of core histone tails with nucleosomal DNA following acetylation and transcription factor binding, *Mol. Cell. Biol. 18*, 6293−6304.
29. Cotten, M., and Chalkley, R. (1985) Hyperacetylated histones facilitate chromatin assembly in vitro, *Nucleic Acids Res. 13*, 401−414.
30. Krajewski, W. A. (2002) Histone acetylation status and DNA sequence modulate ATP-dependent nucleosome repositioning, *J. Biol. Chem. 277*, 14509−14513.
31. Krajewski, W. A., and Becker, P. B. (1998) Reconstitution of hyperacetylated, DNase I-sensitive chromatin characterized by high conformational flexibility of nucleosomal DNA, *Proc. Natl. Acad. Sci. U.S.A. 95*, 1540−5.
32. Levenstein, M. E., and Kadonaga, J. T. (2002) Biochemical analysis of chromatin containing recombinant *Drosophila* core histones, *J. Biol. Chem. 277*, 8749−8754.
33. Krajewski, W. A. (2000) Histone hyperacetylation facilitates chromatin remodelling in a *Drosophila* embryo cell-free system, *Mol. Gen. Genet. 263*, 38−47.
34. Anderson, J. D., Lowary, P. T., and Widom, J. (2001) Effects of histone acetylation on the equilibrium accessibility of nucleosomal DNA target sites, *J. Mol. Biol. 307*, 977−985.
35. Luger, K., Mäder, A. W., Richmond, R. K., Sargent, D. F., and Richmond, T. J. (1997) Crystal structure of the nucleosome core particle at 2.8 Å resolution, *Nature 389*, 251−260.
36. Luger, K., Rechsteiner, T. J., and Richmond, T. J. (1999) Expression and purification of recombinant histones and nucleosome reconstitution, *Methods Mol. Biol. 119*, 1−16.
37. Krajewski, W. A., and Becker, P. B. (1999) Reconstitution and analysis of hyperacetylated chromatin, *Methods Mol. Biol. 119*, 207−217.
38. McMurray, C. T., Small, E. W., and van Holde, K. E. (1991) Binding of ethidium to the nucleosome core particle. Internal and external binding modes, *Biochemistry 30*, 5644−5652.
39. Dorigo, B., Schalch, T., Kulangara, A., Duda, S., Schroeder, R. R., and Richmond, T. J. (2004) Nucleosome arrays reveal the two-start organization of the chromatin fiber, *Science 306*, 1571−1573.
40. Schalch, T., Duda, S., Sargent, D. F., and Richmond, T. J. (2005) X-ray structure of a tetranucleosome and its implications for the chromatin fibre, *Nature 436*, 138−141.
41. Cotton, R. W., and Hamkalo, B. A. (1981) Nucleosome dissociation at physiological ionic strengths, *Nucleic Acids Res. 9*, 445−457.
42. Resemann, A., Suckau, D., Dormeyer, W., Tóth, K., and Schnölzer, M. (2005) Top-down sequence and modification analysis of histones using reISD and T3-sequencing, in *ASMS Conference on Mass Spectrometry and Allied Topics*, San Antonio, TX.
43. Meersseman, G., Pennings, S., and Bradbury, E. M. (1992) Mobile nucleosomes—a general behavior, *EMBO J. 11*, 2951−2959.

BI052110U